



ELSEVIER

Contents lists available at ScienceDirect

## Journal of Magnetism and Magnetic Materials

journal homepage: [www.elsevier.com/locate/jmmm](http://www.elsevier.com/locate/jmmm)

# The manifestations of the two-dimensional magnetic correlations in the nanocrystalline ribbons $\text{Fe}_{64}\text{Co}_{21}\text{B}_{15}$

R.S. Iskhakov<sup>a,c</sup>, S.V. Komogortsev<sup>a,c,\*</sup>, A.D. Balaev<sup>a</sup>, A.A. Gavriluk<sup>b</sup><sup>a</sup> Kirensky Institute of Physics, SB RAS, Krasnoyarsk, Russia<sup>b</sup> Irkutsk State University, Irkutsk, Russia<sup>c</sup> Siberian State Technological University, Krasnoyarsk, Russia

## ARTICLE INFO

## Article history:

Received 9 June 2014

Received in revised form

8 August 2014

Available online 28 August 2014

## Keywords:

Magnetic correlations

Nanocrystalline alloys

Random magnetic anisotropy

Coercivity

## ABSTRACT

We report and discuss the grain size dependence of the coercivity and approach magnetization to saturation in the FeCoB ribbons. Instead of expected three-dimensional magnetic correlations for 20  $\mu\text{m}$  thick ribbon with grain size about 10 nm, the observed behavior could be attributed to the two-dimensional stochastic magnetic domains and two dimensional magnetization ripple.

© 2014 Elsevier B.V. All rights reserved.

## 1. Introduction

Magnetic behavior in the nanocrystalline alloys shows power-law dependence of the coercive force  $H_c$  on the crystallite size  $H_c \sim D^n$  [1–4]. This dependence implies sharp increase in  $H_c$  with the grain size, while the grain growth in coarse-grained materials leads to the decrease of  $H_c$ . The  $H_c \sim D^6$  behavior was first observed in the Finemet alloy [1] and has attracted considerable attention. This behavior was also experimentally found in many other alloys [4–6] and is now incorporated into modern textbooks on magnetism [7–9].

The power-law dependence of the coercive force on the grain size is described by the random magnetic anisotropy (RMA) model [1–4,10–12]. According to this model, the magnetic structure of an amorphous or a nanocrystalline magnetic alloy is an ensemble of the stochastic magnetic domains spread over a large amount of particles with random orientation of the easy magnetization axis [1,13]. Coercivity and susceptibility both depend on the value of the effective anisotropy of these domains, and the latter depends strongly on the domain size. The important result of the RMA model is the power-law dependence of the magnetic anisotropy in the stochastic magnetic domain on the crystallite size:  $\langle K \rangle \sim D^n$  [1–4,14,15]. This dependence causes the power-law grain-size dependence of the coercive force and the ferromagnetic resonance line-width in nanocrystalline alloys [1–6,16,17]. However, the exponent  $n$  in the empirically established power-law grain size dependence of  $H_c(D)$  sometimes differs from 6. The exponents

ranging from 1.5 to 6 are found [1–6,18–24]. It is still unclear whether the value of the exponent below 6 should be attributed to the induced uniaxial anisotropy [18] or to the reduced dimensionality of the stochastic magnetic domain ( $d$ ) [19–21] taking into account one of the results of the RMA model  $n = 2d/(4-d)$  [14,15]. So, experimental studies of the grain-size dependence of the coercivity in nanocrystalline alloys should be performed in order to clarify the problem. In this paper, we present experimental results on the grain size dependence of the coercive force and the approach magnetization to saturation in nanocrystalline alloy ribbons  $\text{Fe}_{64}\text{Co}_{21}\text{B}_{15}$  obtained by annealing the amorphous alloy.

## 2. Experiment

Initial melt quenched 20  $\mu\text{m}$  thick ribbon  $\text{Fe}_{64}\text{Co}_{21}\text{B}_{15}$  is amorphous. The ribbon was cut into small samples which then were annealed for one hour at different temperatures up to 480 °C in the argon atmosphere. Magnetization curves were measured at room temperature by the vibrating sample magnetometer in the fields up to 800  $\text{kA m}^{-1}$  applied along the ribbon plane. X-ray powder diffraction (XRD) patterns were measured by the DRON-3 using  $\text{Cu K}\alpha$  radiation. Phase determination was carried out using the powder diffraction database [25].

## 3. Results and discussion

The XRD pattern for the initial sample  $\text{Fe}_{64}\text{Co}_{21}\text{B}_{15}$  and the sample annealed at 200 °C is the wide halo characteristic of the amorphous state (Fig. 1). Annealing at 300 °C leads to the emergence of the clear

\* Corresponding author.

E-mail address: [komogor@iph.krasn.ru](mailto:komogor@iph.krasn.ru) (S.V. Komogortsev).

bcc phase Fe–Co reflections on the amorphous halo. Further annealing leads to the appearance of the reflections of the two base centered tetragonal (bct) phases—(Fe,Co)<sub>3</sub>B and (Fe,Co)<sub>2</sub>B. However, these reflections are weak compared to the bcc reflexes, so the amount of these phases in the annealed samples is small relative to the bcc phase.

Full width at the half maximum (FWHM) for the bcc phase reflections decreases with annealing temperature due to grain growth. We estimate the crystallite size ( $D$ ) by the Scherrer formula  $D=0.9 \cdot \lambda/(\text{FWHM} \cdot \cos(\theta))$  for the bcc phase using the position ( $2\theta$ ) and FWHM of the most intensive peak (0 1 1). The profile of the peak was fitted by the pseudo-Voigt function to determine the FWHM accurately.

The hysteresis loop shape changes during annealing (inset in Fig. 2). The magnetization measured at 1 T increases from

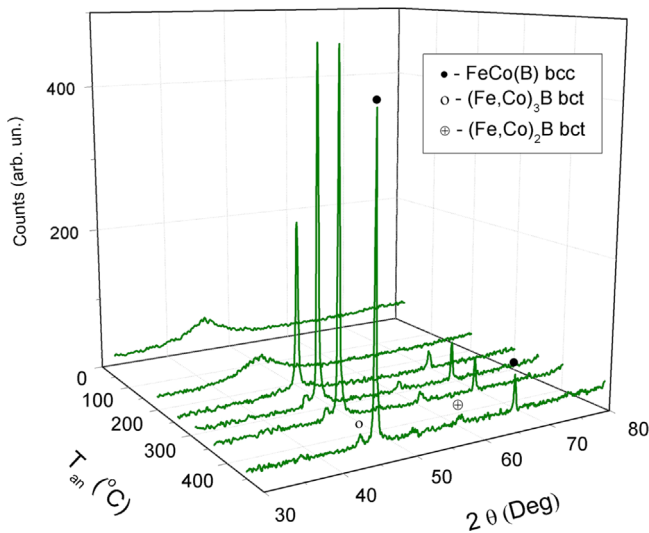


Fig. 1. X-ray powder diffraction pattern of FeCoB ribbons: as-prepared and annealed during 1 h at different temperatures.

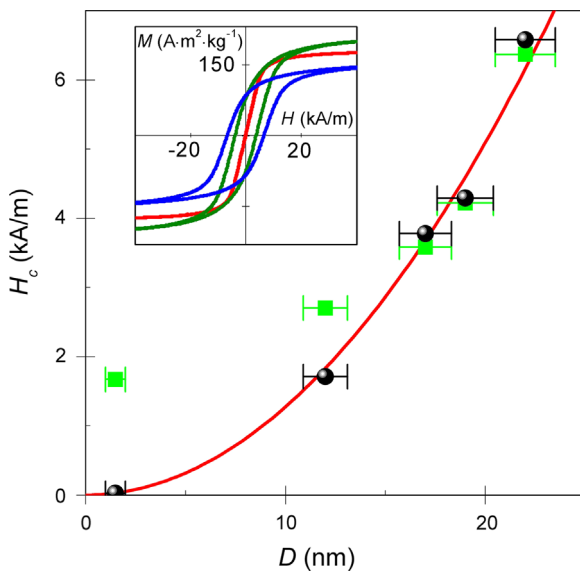


Fig. 2. Grain size dependence of the coercivity in the FeCoB ribbons (the black spheres—coercivity  $H_c$ ; the green boxes— $b = (a^2/\epsilon) \times (H_a)$ ; the solid line— $H_c = 0.0127 \times D^2$ ). The inset show hysteresis loops for the as-prepared (red and moderate  $M_s$ ) and annealed during 1 h at 350 °C (green and maximal  $M_s$ ) and 480 °C (blue and lowest  $M_s$ ) samples. (For interpretation of the references to color in this figure legend, the reader is referred to the web version of this article.)

182 A m<sup>2</sup> kg<sup>−1</sup> for the amorphous alloy to 217 A m<sup>2</sup> kg<sup>−1</sup> for the annealed at 300 and 350 °C samples. Further annealing results in the magnetization decrease to 165 A m<sup>2</sup> kg<sup>−1</sup> for  $T_{\text{an}} = 480$  °C. The change of the magnetization reflects the evolution of the phase content. The solid solution of bcc FeCo(B) with the highest magnetization is formed at the initial stages of annealing. Then the tetragonal iron borides with lower magnetization are formed.

The coercive force and the grain size of the bcc solid solution phase FeCo(B) increase significantly during annealing (inset Fig. 2). Coercive force  $H_c$  and the grain size  $D$  correlate. Allometric fitting by  $H_c(D) = aD^n$  gives the exponent  $n = 2.2 \pm 0.2$  that is very close to the 2 in the simple quadratic dependence  $H_c \sim D^2$ . This dependence  $H_c \sim D^2$  fits the data in Fig. 2 very well and we will further discuss it. The observed  $H_c \sim D^2$  dependence is inconsistent both with the  $H_c \sim D^6$  law for the nanocrystalline alloys with the three dimensional nanostructure and the three dimensional stochastic magnetic domains [1–6] and with the widely discussed recently  $H_c \sim D^3$  dependence for alloys with the induced uniaxial magnetic anisotropy [18]. According to [15,19–21,26] the exponent 2 can be attributed to the two-dimensional stochastic magnetic domains formed in the alloy. The two-dimensional stochastic magnetic domains are expected to be found in magnetic films with thickness comparable to the crystallite size. In our case we deal with the 20 μm thick ribbon whose crystallite size is about 10–20 nm which should be expected to form the three dimensional stochastic magnetic domains with the size ranging from 0.1 to 1 μm in the amorphous ribbon [13].

The magnetization approaches saturation as  $M(H) = M_s \times (1 - b/H)$  (Fig. 3) in the range from 80 to 800 kA m<sup>−1</sup>, where  $b$  value increases with the annealing temperature. According the RMA model this dependence implies two dimensional magnetic correlations (two dimensional magnetization ripple) in the sample or two dimensional structural inhomogeneity [13,15,26–31]. We thus have two manifestations of the two dimensional magnetic correlations in the ribbon with the three dimensional nanostructure: (1) the grain size dependence of the coercivity (Fig. 2) and (2) the approach of magnetization to saturation in the ribbon. The dependence  $\Delta M/M_s \sim H^{-1}$  in the thick coatings and rapidly quenched ribbons with the thickness of several tens of microns has been observed by many groups [13,17,32–36]. This may indicate that two dimensional magnetic or structural heterogeneity is the common feature of the nanocrystalline and amorphous ribbons. The key parameter of the RMA model in the high fields is the magnetic correlation length  $R_H = \sqrt{2A/(M_s H)}$ . It is constrained by the condition  $R_c \leq R_H \leq R_L$ , where  $R_c$  is the structural correlation

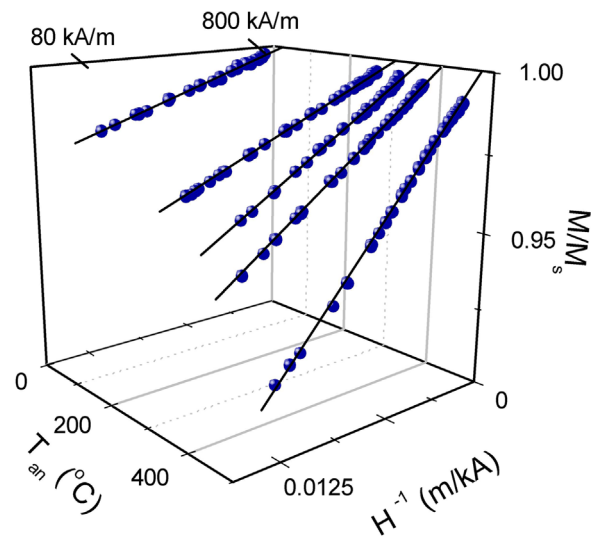


Fig. 3. Approach magnetization to saturation in FeCoB ribbons.

length or the grain size and  $R_L$  is the stochastic magnetic domain size. In this range magnetization approaches saturation according to  $\Delta M/M_s \sim H^{-(4-d)/2}$  [13,15,28,29]. The applied field range corresponding to the constraint  $R_c \leq R_H \leq R_L$  is  $H_L \leq H \leq H_R$  where  $H_R = 2A/(M_s R_c^2)$  and  $H_L = 2A/(M_s R_L^2)$ . In the nanostructured ribbons the structural correlation length may be anisotropic: normal out-of-plane component  $R_c^\perp$  and in-plane component  $R_c^\parallel$  may differ. In case of  $R_c^\perp < \sqrt{A/\epsilon K} < R_c^\parallel$ , where  $\epsilon$  is the dimensionless parameter less than unity [13,37], the magnetic correlations will spread only along the ribbon plane and thus will be two dimensional. It may explain our observations in Figs. 2 and 3 which indicate two dimensional magnetic correlations in the nanocrystalline ribbon with the three dimensional nanostructure.

The above interpretation is supported by the grain size dependence of the coefficient  $b$  determined from the approach magnetization to saturation curves (Fig. 3). The point is that the  $b$  value is closely tied to the average magnetic anisotropy field in stochastic magnetic domain  $\langle H_a \rangle$ :  $b = (a^2/\epsilon) \times \langle H_a \rangle$ , where  $a$  is a symmetry related coefficient equal to  $1/15^{1/2}$  in case of the uniaxial random anisotropy [13,27]. Assuming that the symmetry of the magnetic anisotropy and the coefficient  $\epsilon$  are constant during annealing, and that the  $H_c$  is proportional to the magnetic anisotropy field  $\langle H_a \rangle$  one can expect the direct correlation of  $H_c$  and  $b$  values. The value of  $b$  and coercive field  $H_c$  determined from the hysteresis loops with  $M_r/M_s$  about 0.5 are close to each other. The correspondence between  $H_c$  and  $(a^2/\epsilon) \times \langle H_a \rangle$  is consistent with the point that if the hysteresis loop shape is determined mainly by the random magnetic anisotropy, the remanence  $M_r/M_s$  should be close to the prediction of the Stoner–Wohlfarth model  $M_r/M_s = 0.5$  [3,38,39]. Using another result of the Stoner–Wohlfarth model  $H_c = \langle H_a \rangle/2$ , and the good agreement between  $(a^2/\epsilon) \times \langle H_a \rangle$  and  $H_c$  we estimate the coefficient  $(a^2/\epsilon)$  to be  $a^2/\epsilon \approx 1/2$ .

The anisotropy of the structural correlation length  $R_c^\perp \neq R_c^\parallel$  could explain the observed experimental data qualitatively. Quantitative estimations could be made in the following way. The discussion points out to the constraints  $R_c^\perp < \sqrt{A/\epsilon K} < R_c^\parallel$  and allows us to estimate the aspect ratio  $R_c^\perp/R_c^\parallel \leq (H_L/H_R)^{1/2}$ . In our case, the  $H_L$  and  $H_R$  values can be estimated using the lower and the upper limits in the range of fields where the  $\Delta M \sim H^{-1}$  dependence is observed ( $H_L < 80 \text{ kA m}^{-1}$  and  $H_R > 800 \text{ kA m}^{-1}$ ), from which we estimate  $R_c^\perp/R_c^\parallel \leq 0.32$ . The low dimensional inhomogeneity of the magnetic anisotropy in the amorphous and nanocrystalline alloys could arise from structural defects caused by the symmetry of the temperature gradient during the rapid quenching of ribbons [40], or by the intrinsic features of the amorphous alloy such as the elastic [41] and the compositional low dimensional inhomogeneity [42,43].

#### 4. Conclusions

The manifestations of the two-dimensional magnetic correlations were observed in the ribbons of the amorphous and nanocrystalline alloys  $\text{Fe}_{64}\text{Co}_{21}\text{B}_{15}$ . The first clue is the approach of magnetization to saturation:  $\Delta M \sim H^{-1}$ , which implies a two-dimensional spread of the magnetic correlations in the fields ranging from 80 to 800  $\text{kA m}^{-1}$ . The second clue is the quadratic dependence of the coercive force  $H_c$  on the grain size  $H_c \sim D^2$ , which is characteristic of the two-dimensional stochastic magnetic domains formation in the fields close to the  $H_c$  value. This indicates that the structural correlation length is anisotropic ( $R_c^\perp \neq R_c^\parallel$ ) and allows us to estimate the ratio  $R_c^\perp/R_c^\parallel$  (in this case less than 0.32). These results are useful in the optimization of the atomic and magnetic microstructure of the amorphous and nanocrystalline ferromagnetic alloys and allows to create novel soft magnetic materials.

#### References

- [1] G. Herzer, Grain size dependence of coercivity and permeability in nanocrystalline ferromagnets, IEEE Trans. Magn. 26 (1990) 1397–1402.
- [2] G. Herzer, Nanocrystalline soft magnetic materials, J. Magn. Magn. Mater. 157–158 (1996) 133–136.
- [3] G. Herzer, Anisotropies in soft magnetic nanocrystalline alloys, J. Magn. Magn. Mater. 294 (2005) 99–106.
- [4] G. Herzer, Modern soft magnets: amorphous and nanocrystalline materials, Acta Mater. 61 (2013) 718–734.
- [5] M. Müller, N. Mattern, U. Kühn, Correlation between magnetic and structural properties of nanocrystalline soft magnetic alloys, J. Magn. Magn. Mater. 157–158 (1996) 209–210.
- [6] E. Kita, N. Tsukuhara, H. Sato, K. Ota, H. Yangaiharu, H. Tanimoto, et al., Structure and random anisotropy in single-phase Ni nanocrystals, Appl. Phys. Lett. 88 (2006) 152501.
- [7] G. Herzer, Nanocrystalline soft magnetic alloys, in: K.H.J. Buschow (Ed.), Handb. Magn. Mater., Amsterdam, 1997: pp. 415–462.
- [8] R. Hilzinger, Applications of nanocrystalline soft magnetic materials, in: B. Cantor (Ed.), Nov. Nanocrystalline Alloy. Magn. Nanomater, CRC Press, Bristol, 2004, p. 325.
- [9] G. Herzer, Soft Magnetic Materials—Nanocrystalline Alloys, in: H. Kronmüller, S. Parkin (Eds.), Handb. Magn. Adv. Magn. Mater. V. 4 Nov. Mater., John Wiley & Sons, Ltd, Chichester, UK, 2007, pp. 1–25.
- [10] V.A. Ignatchenko, R.S. Iskhakov, Spin waves in stochastic anisotropic materials, J. Exp. Theor. Phys. 45 (1977) 526–533.
- [11] V.A. Ignatchenko, R.S. Iskhakov, Stochastic magnetic structure and spin waves in amorphous ferromagnetic substance, Izv. Akad. Nauk SSSR, Ser. Fiz. 44 (1980) 1434.
- [12] R. Alben, J.J. Becker, M.C. Chi, Random anisotropy in amorphous ferromagnets, J. Appl. Phys. 49 (1978) 1653.
- [13] R.S. Iskhakov, S.V. Komogortsev, Magnetic microstructure of amorphous, nanocrystalline, and nanophase ferromagnets, Phys. Met. Metall 112 (2011) 666–681.
- [14] G. Herzer, Magnetization process in nanocrystalline ferromagnets, Mater. Sci. Eng., A 133 (1991) 1–5.
- [15] R.S. Iskhakov, S.V. Komogortsev, A.D. Balaev, L.A. Chekanova, Dimensionality of a system of exchange-coupled grains and magnetic properties of nanocrystalline and amorphous ferromagnets, J. Exp. Theor. Phys. Lett 72 (2000) 304–307.
- [16] S.V. Komogortsev, R.S. Iskhakov, P.A. Kuznetsov, A.I. Belyaeva, G.N. Bondarenko, L.A. Chekanova, Properties of ferromagnetic resonance in  $\text{Fe}_{73.5}\text{CuNb}_{3.5}\text{Si}_{13.5}\text{B}_9$  nanocrystalline alloys, Phys. Solid State 52 (2010) 2287–2290.
- [17] S.V. Komogortsev, R.S. Iskhakov, P.A. Kuznetsov, A.I. Belyaeva, G.N. Bondarenko, L.A. Chekanova, et al., Random magnetic anisotropy and ferromagnetic resonance in nanocrystalline alloy  $\text{Fe}_{73.5}\text{CuNb}_{3.5}\text{Si}_{13.5}\text{B}_9$ , Solid State Phenom. 168–169 (2011) 365–368.
- [18] K. Suzuki, G. Herzer, Magnetic-field-induced anisotropies and exchange softening in Fe-rich nanocrystalline soft magnetic alloys, Scr. Mater 67 (2012) 548–553.
- [19] S. Thomas, S.H. Al-Harhi, D. Sakthikumar, I.A. Al-Omari, R.V. Ramanujan, Y. Yoshida, et al., Microstructure and random magnetic anisotropy in Fe–Ni based nanocrystalline thin films, J. Phys. D: Appl. Phys 41 (2008) 155009.
- [20] J. Echigoya, R. Yue, Grain-size dependence of coercive force in sputtered and annealed iron films, J. Mater. Sci. 40 (2005) 3209–3212.
- [21] M.C. Contreras, J.F. Calleja, R. Matarranz, B. Presa, J.A. Corrales, G. Pan, Effect of grain size on the soft magnetic properties of  $\text{FeCoV}/\text{CoNbZr}$  multilayers, J. Appl. Phys. 99 (2006) 08F110.
- [22] N. Turriza, N. Murillo, J.J. del Val, J. González, G. Vara, A.R. Pierna, Nanocrystallization by current annealing (with and without tensile stress) of  $\text{Fe}[\text{sub } 73.5-x][\text{Ni}[\text{sub } x][\text{Si}[\text{sub } 13.5][\text{B}[\text{sub } 9][\text{Nb}[\text{sub } 3][\text{Cu}[\text{sub } 1]]] alloy ribbons ( $x=5, 10$ , and  $20$ ), J. Appl. Phys 103 (2008) 113904.$
- [23] N. Murillo, J. González, Effect of the annealing conditions and grain size on the soft magnetic character of  $\text{FeCu}(\text{Nb}/\text{Ta})\text{SiB}$  nanocrystalline alloys, J. Magn. Magn. Mater. 218 (2000) 53–59.
- [24] S. Joshi, S.D. Yoon, A. Yang, N.X. Sun, C. Vittoria, V.G. Harris, et al., Structure and magnetism of nanocrystalline exchange-coupled  $(\text{Ni}[\text{sub } 0.67][\text{Co}[\text{sub } 0.25][\text{Fe}[\text{sub } 0.08]][\text{sub } 89-x][\text{Zr}[\text{sub } 7][\text{B}[\text{sub } 4][\text{Cu}[\text{sub } x]]]$  ( $x=0.1$ ) films, J. Appl. Phys. 99 (2006) 08F115.
- [25] JCPDS X-ray Diffraction Data Card File and Key, 1997.
- [26] R.S. Iskhakov, S.V. Komogortsev, A.D. Balaev, L.A. Chekanova, Multilayer  $\text{Co}/\text{Pd}$  films with nanocrystalline and amorphous Co layers: coercive force, random anisotropy, and exchange coupling of grains, Tech. Phys. Lett. 28 (2002) 725–728.
- [27] E.M. Chudnovsky, A theory of two-dimensional amorphous ferromagnet, J. Magn. Magn. Mater. 40 (1983) 21–26.
- [28] V.A. Ignatchenko, R.S. Iskhakov, The magnetization curve of ferromagnets with anisotropic and low-dimensional inhomogeneities, Fiz. Met. Metalloved 73 (1992) 602–608.
- [29] R.S. Iskhakov, V.A. Ignatchenko, S.V. Komogortsev, A.D. Balaev, Study of magnetic correlations in nanostructured ferromagnets by correlation magnetometry, J. Exp. Theor. Phys. Lett 78 (2003) 646–650.
- [30] C. Binns, M.J. Maher, Magnetic behaviour of thin films produced by depositing pre-formed Fe and Co nanoclusters, New J. Phys. 4 (2002) (85–85).

- [31] J. Ruiz, X. Zhang, C. Ferrater, J. Tejada, Evidence of extended orientational order in amorphous Fe/Sm thin films, *Phys. Rev. B: Condens. Matter* 52 (1995) 10202–10206.
- [32] A. Michels, R.N. Viswanath, J.G. Barker, R. Birringer, J. Weissmüller, Range of magnetic correlations in nanocrystalline soft magnets, *Phys. Rev. Lett.* 91 (2003) 267204.
- [33] P. Garoche, A. Malozemoff, Approach to magnetic saturation in sputtered amorphous films: effects of structural defects, microscopic anisotropy, and surface roughness, *Phys. Rev. B: Condens. Matter* 29 (1984) 226–231.
- [34] T. Bitoh, A. Makino, A. Inoue, Origin of low coercivity of  $(\text{Fe}_{0.75}\text{B}_{0.15}\text{Si}_{0.10})_{100-x}\text{Nb}_x$  ( $x=1-4$ ) glassy alloys, *J. Appl. Phys.* 99 (2006) 08F102.
- [35] A. Neuweiler, B. Hofmann, H. Kronmüller, Approach to magnetic saturation in nanocrystalline and amorphous Fe<sub>73.5</sub>Cu<sub>1</sub>Nb<sub>3</sub>Si<sub>13.5</sub>B<sub>9</sub>, *J. Magn. Magn. Mater.* 153 (1996) 28–34.
- [36] X.Y. Xiong, T.R. Finlayson, B.C. Muddle, The approach to saturation magnetization of nanocrystalline Fe<sub>90</sub>Zr<sub>7</sub>B<sub>3</sub> alloy, *J. Phys. D: Appl. Phys.* 34 (2001) 2845–2853.
- [37] R.S. Iskhakov, S.V. Komogortsev, Magnetic microstructure of nanostructured ferromagnets, *Bull. Russ. Acad. Sci. Phys* 71 (2007) 1620–1622.
- [38] S. Flohrer, G. Herzer, Random and uniform anisotropy in soft magnetic nanocrystalline alloys (invited), *J. Magn. Magn. Mater.* 322 (2010) 1511–1514.
- [39] E.C. Stoner, E.P. Wohlfarth, A mechanism of magnetic hysteresis in heterogeneous alloys, *Philos. Trans. R. Soc. London, Ser. A* 240 (1948) 559.
- [40] G.E. Abrosimova, Evolution of the structure of amorphous alloys, *Physics-Uspeski* 54 (2011) 1227–1242.
- [41] H. Kronmüller, Micromagnetism and microstructure of amorphous alloys (invited), *J. Appl. Phys.* 52 (1981) 1859–1864.
- [42] K.G. Pradeep, G. Herzer, P. Choi, D. Raabe, Atom probe tomography study of ultrahigh nanocrystallization rates in FeSiNbBCu soft magnetic amorphous alloys on rapid annealing, *Acta Mater.* 68 (2014) 295–309.
- [43] M.J. Duarte, A. Kostka, J.A. Jimenez, P. Choi, J. Klemm, D. Crespo, et al., Crystallization, phase evolution and corrosion of Fe-based metallic glasses: an atomic-scale structural and chemical characterization study, *Acta Mater.* 71 (2014) 20–30.